

HIGH TEMPERATURE ELECTROCHEMICAL CORROSION RATE PROBES

Sophie J. Bullard, Bernard S. Covino, Jr., Gordon R. Holcomb,
and Margaret Ziomek-Moroz
U.S. Department of Energy
Albany Research Center
1450 Queen Ave., SW
Albany, OR 97321

ABSTRACT

Corrosion occurs in the high temperature sections of energy production plants due to a number of factors: ash deposition, coal composition, thermal gradients, and low NO_x conditions, among others. Electrochemical corrosion rate (ECR) probes have been shown to operate in high temperature gaseous environments that are similar to those found in fossil fuel combustors. ECR probes are rarely used in energy production plants at the present time, but if they were more fully understood, corrosion could become a process variable at the control of plant operators.

Research is being conducted to understand the nature of these probes. Factors being considered are: values selected for the Stern-Geary constant, the effect of internal corrosion, and the presence of conductive corrosion scales and ash deposits. The nature of ECR probes will be explored in a number of different atmospheres and with different electrolytes (ash and corrosion product). Corrosion rates measured using an electrochemical multi-technique capabilities instrument will be compared to those measured using the linear polarization resistance (LPR) technique. In future experiments, electrochemical corrosion rates will be compared to penetration corrosion rates determined using optical profilometry measurements.

OBJECTIVE

The research aims to show that electrochemical corrosion rate (ECR) probes are viable for use in fossil fuel energy conversion systems and that they provide added value. These probes will be able to be used to continuously monitor corrosion rates of key Power Plant components and associate changes in corrosion behavior with other process changes. Corrosion rate can become a process variable for Power Plants. ECR probes can also be used to track corrosion losses of key components in order to more efficiently schedule downtime for maintenance activities. A number of research efforts have been aimed at developing high temperature corrosion probes for various industries. The majority of the research has been based on the use of electrochemical noise (EN)¹⁻⁷ techniques. Others have considered the use of electrochemical impedance spectroscopy (EIS)³⁻⁵ and linear polarization resistance (LPR)⁶, zero resistance ammetry (ZRA)⁴, and electrical resistance (ER)⁴. However, only a limited effort has been made to quantify the operation of corrosion rate probes. For these probes to be accepted routinely in the power generation industries, it will be necessary to determine if they accurately measure corrosion and the changes in corrosion rate that occur in environments of interest, if the sensor materials

have an optimum composition for the intended exposure, and if the sensitivity or accuracy of the sensor changes with exposure time in fireside environments. Once this is established, electrochemical corrosion rate sensors can be used extensively and will allow corrosion rate to become a process variable for power plant operators. Most electrochemical corrosion rate measurement techniques measure a resistance that is representative of the rate of the corrosion reaction. This is true of the LPR, EN, and EIS techniques. These resistances are related to corrosion rate by the Stern-Geary linear approximation to the Butler-Volmer equation:

$$R_p = R_n = \frac{\Delta E}{\Delta i_{\text{applied}}} = \frac{\beta_a \beta_c}{2.303(i_{\text{corr}})(\beta_a + \beta_c)} = \frac{B}{(i_{\text{corr}})} \quad (1)$$

where R_p is a resistance obtained from the LPR and EIS techniques, R_n is a resistance obtained from the EN technique, ΔE is the incremental change in potential measured due to the incremental change in applied current density, $\Delta i_{\text{applied}}$, B is the Stern-Geary constant, β_a and β_c are the anodic and cathodic Tafel constants, respectively, and i_{corr} is the corrosion current density from which a corrosion rate may be calculated using Faraday's Law. The Stern-Geary constant (determined by the Tafel constants) is the only variable that is normally not measured, but commonly assumed to be a value of 0.020 to 0.030 V/decade. Because B is related to Tafel constants, it can be measured using either standard electrochemical polarization techniques or the harmonic distortion analysis (HDA) technique that is used in this report.

EXPERIMENTAL DETAILS

ECR Probe Construction

Isothermal probes are exposed nominally to the same temperature as the environment. These can be made as single or multi-probes. Multi-probes allow for increased amount of data for each experiment, where different alloys or different ashes can be exposed simultaneously in the same experiment.

A cylindrical piece of ceramic served as the form to contain the sensors. Sensors were embedded within the ceramic form first using alumina cement and later using Ceramcast 586, a zirconia/magnesia potting compound. The stainless steel tubing served to isolate the wires from the test environment and provided a path for the wires to exit the high temperature environment. After curing at room temperature for 12 to 18 hours, the ECR probe was cured at 93°C for 4 hours and then at 121°C for 3 hours. The finished



Figure 1 — ECR isothermal probe covered with ash.

probe is shown in Figure 1.

Probes built and used to date were built for use in laboratory tube furnaces. Probes to be tested in future experiments are air cooled probes contain a cooling chamber that allows the use of liquids or gases to adjust the temperature of the metallic sensors to a temperature of interest. Figure 2 shows an air-cooled probe. Air cooled probes consist of three sensors with electrical leads, an air chamber, stainless steel tubes to carry air into and out of the chamber, a type K thermocouple at the outer surface of the probe, and a type K



Figure 2 – Photo of a air-cooled ECR probe

thermocouple within the air chamber. These thermocouples are intended to give the adjusted sensor temperatures and the thermal gradient across the sensors. The air chamber is made by casting a cube of Styrofoam within the sensor adjacent to the back of the sensors and then removing that cube using acetone to dissolve it after the potting compound hardens.

Isothermal probes are identical to the air-cooled probe without the thermocouples, air chamber, and air tubes. Multi-probes are made by combining up to three isothermal probes together in series. Each probe has separate electrical leads to their respective sensors. Probes intended for use in field tests will incorporate features of the laboratory probes but also will need to be more rugged to survive the actual industrial environment.

EXPERIMENTAL DESIGN

Hardware/Software Systems

The hardware used to measure the majority of the corrosion rates from the ECR probes is the SmartCET[®] Corrosion Monitoring System. This system used three separate electrochemical techniques: linear polarization resistance (LPR), electrochemical noise (EN), and harmonic distortion analysis (HDA). All three techniques measure a corrosion rate, EN also measures a localized (pitting) corrosion factor that varies from 0 to 1, and HDA measures the Tafel (β_a and β_c) and Stern-Geary (B) Constants. Corrosion rates and other variables are reported every 7 minutes and stored to computer using FieldCET[®] software. All corrosion rates in this report are taken from the LPR measurements modified using the measured B values from each experiment.

Alternative electrochemical measurements were made using a PAR 273A potentiostat/galvanostat. Potentiodynamic polarization tests were conducted at 0.167 mV/s from -0.2 V vs open circuit potential (OCP) to +0.5 V vs OCP. When pitting

corrosion was suspected, the potential was reversed at +0.5 V vs OCP and scanned to -0.2V vs OCP. LPR measurements were made at 0.167 V/s from -15 mV to +15 mV vs OCP. All electrochemical measurements were controlled using DC Corrware software.

Research Apparatus

All experiments were conducted in a 3-zone tube furnace containing a 2 in diameter alumina tube. Each zone was controlled with a separate temperature controller. Set temperatures for each zone were determined for each test temperature using an external calibration thermocouple and taking measurements at 1 in intervals. For example, settings of 490, 510, and 400°C for zones 1, 2, and 3, respectively, gives an internal temperature of 500°C with a flat profile over 12 in of the 24 in heated zone. An alumina D-tube is inserted in the furnace tube to allow a platform for mass loss coupons. Measurement and control thermocouples are inserted in a 316 SS sheath that is then inserted in the D-tube.

Gas flows were controlled using digital mass flow controllers that are controlled using Labview programs. Water vapor is added through an air-powered metering pump that pumped a specific quantity of water into a heated chamber through which the test gas flowed.

RESULTS AND DISCUSSION

ECR Probe Response

A 500 h exposure test for an incinerator ash-coated 304 SS ECR probe in a N₂/O₂/CO₂ gaseous environment was conducted to show the effect of gas composition changes on probe response. The probe was heated to temperature in N₂ and allowed to remain in N₂ for about 165 hrs. During this time the corrosion rate remained high at 4-5 mm/y, decreasing slightly. After 165 hours, the gas composition was changed to N₂/O₂/CO₂ which caused the corrosion rate to begin a decrease to about 1 mm/y at 230 h. Here the gas was again switched to N₂ which again caused the corrosion rate to increase to 4-5 mm/y. After peaking at 4.8 mm/y, the corrosion rate started decreasing. The addition of CO₂ at 250 h continued the decrease in corrosion rate but with a change in slope. The addition of O₂ at 295 h again continued the decrease in corrosion rate with yet another change in slope. This experiment shows that both O₂ and CO₂ cause the corrosion rate of the ash-covered 304 SS to decrease as soon as those gases are present while corrosion rates in N₂ decrease only after an incubation period.

Effect Of Ash Composition

Two different types of ash were used in this research. The first was an ash from the Lee #1 Municipal Incinerator supplied by Covanta Energy, Inc. The second was a coal ash described as AEP TIDD Ash derived from Illinois #8 coal, and supplied by EERC, the University of North Dakota Energy and Environmental Research Center. The composition of the two types of ash are: **Illinois No. 8 Coal Ash:** Al₂O₃ – 7.6%, CaO –

28.3%, K₂O – trace, TiO₂ – trace, MgO – 15.6%, Na₂O – trace, P₂O₅ – trace, Fe₂O₃ – 6.4, SiO₂ – 23.7, SO₃ – 15%. **Incinerator Ash:** Al – 3.63%, Mn – 631 ppm, As – 107 ppm, Ca – 9.97%, K – 3.69%, Pb – 2.7%, Ti – 0.514%, Mg – 0.734%, Na – 3.53%, Cr – 482 ppm, Ag – < 20 ppm, P – 0.213%, Cd – 883 ppm, Se – < 50 ppm, Cl – 6.71%, Left on Ignition, LOI – 26.6%, C – 0.135%, N₂ – 0.171%, Fe – 5%, Si – 8%, S – 6.47

Incinerator ash was used for the majority of the experiments discussed in this report. This ash shows high concentrations of corrosion-causing elements such as S, Cl, Pb, and K, all of which are able to form low melting point compounds and eutectic mixtures. The gas mixture consisted of 68 vol% N₂, 15 vol% H₂O, 9 vol% O₂, and 8 vol% CO₂. Water vapor was sometimes added to the gas stream. Temperatures ranged from 450 to 600°C and typical test periods were 100 to 500 hours.

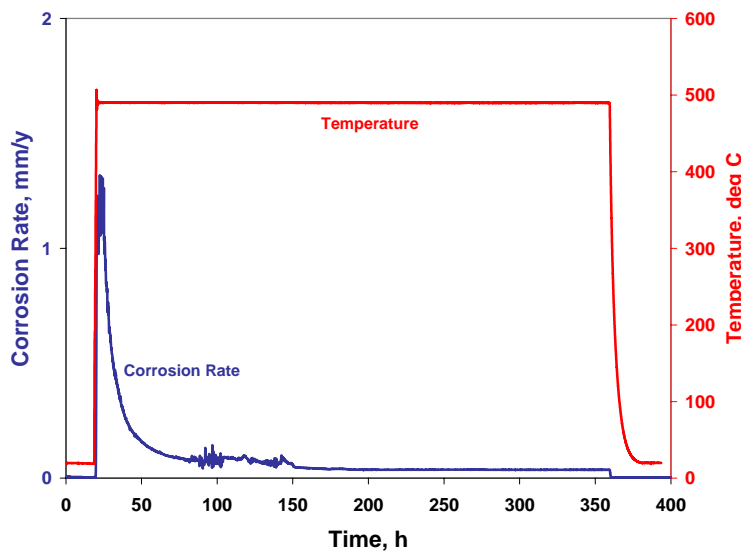


Figure 3 – Corrosion rate response of incinerator- ash-covered ECR Probe at 500°C.

Coal ash was used for one experiment that ran for about 150 h. This ash notably lacks most of the corrosion-causing elements that are present in the incinerator ash. The gas mixture used consisted of 69 vol% N₂, 15 vol% CO₂, 10 vol% H₂O, 5 vol% O₂, and 1 vol% SO₂. Figure 3 shows the typical response of a 304 SS ECR probe coated with incinerator ash. An expansion of the beginning of the experiment would show a

small amount of corrosion when the ash/methanol slurry was applied to the probe before heat-up. The corrosion rate increase was also noted to lag behind the temperature increase until approximately 400°C. Corrosion rate was typically unstable for a period of time after the addition of the experiment environment. After that point the corrosion rate decreased over a period of 50 to 100 h.

Figure 4 shows the typical response of a 304 SS ECR probe coated with coal ash. An expansion of the beginning of the experiment would show a small amount of corrosion when the ash/methanol slurry was applied to the probe before heat-up. Also visible would be the fact that the corrosion rate increase lags behind the temperature increase until approximately 400°C. In coal ash, however, the corrosion rate is much lower at the beginning of the experiment than that shown in Figure 3. Another interesting phenomenon is that when the N₂/CO₂/O₂/SO₂ environment was added, the corrosion rate did not increase. The corrosion rate started increasing 24 h later when water vapor was

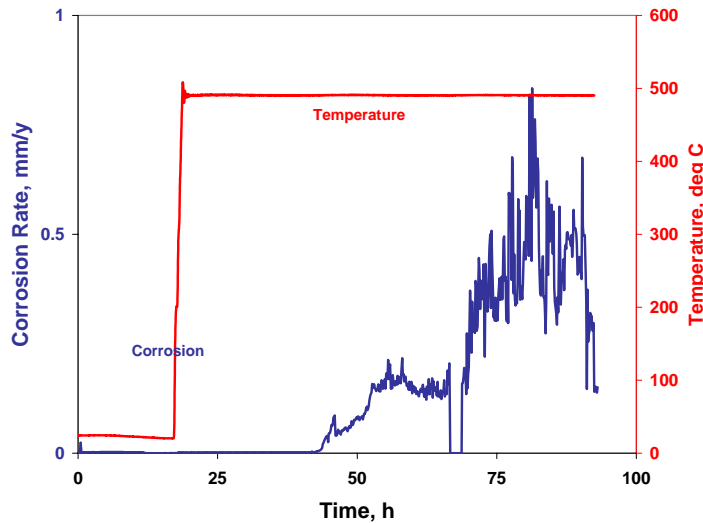


Figure 4 – Corrosion rate response of a coal-ash-covered 304 SS ECR probe at 500°C.

added to the environment. Corrosion rates did not decrease with time as shown in Figure 3 for the incinerator-ash-covered 304 SS ECR probe, but actually increased with time.

The localized corrosion or pitting factor is an indication of the probability of pitting that is reported from the EN technique. The pitting factor (PF) ranges from 0 to 1 but is best divided into logarithmic decades of 0.001 to 0.01 (no probability of localized corrosion), 0.01 to 0.1 (slight probability of

localized corrosion), and 0.1 to 1 (high probability of localized corrosion). In all of the experiments conducted on ECR probes covered with incinerator ash, there was never an indication of the possibility of localized corrosion. This is despite the fact that the incinerator ash contains high levels of chlorides. Results were different for the coal-ash-covered ECR probe. Figure 5 shows the pitting factor to be in the highest range (0.1 to 1) suggesting a high probability of pitting.

Electrochemistry Of The Corrosion Processes On Ash-Covered ECR Probes

Electrochemical measurements were conducted using a standard laboratory potentiostat to verify the accuracy of the SmartCET measurements, to show that other types of equipment can be used reliably to make similar measurements, and to attempt to understand

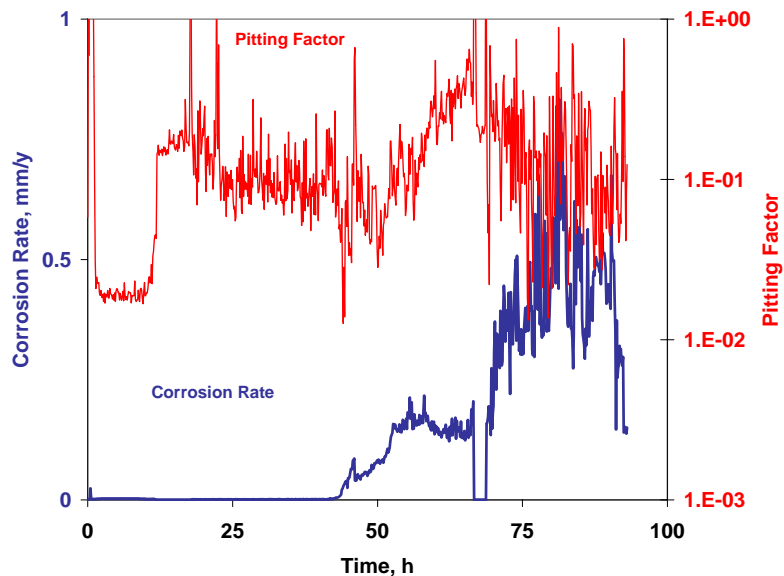


Figure 5 – Corrosion rate and pitting factor as a function of time for a coal-ash-covered 304 SS ECR probe at 500°C.

the electrochemical nature of the corrosion reactions on the ash covered probes. These measurements were taken by interrupting and disconnecting the SmartCET system, allowing the PAR 273A potentiostat to be connected. The potentiodynamic polarization behavior of an incinerator-ash-covered 304 SS ECR probe is shown in Figure 6. This curve is typical of an actively corroding metal and suggests that all or at least some of the corrosion reactions are electrochemical in nature. The linear part of the curve near the corrosion potential in Figure 6 was further analyzed to derive the polarization resistance, R_p . R_p was then converted to a corrosion rate for comparison to the SmartCET LPR corrosion rate. Standard LPR tests were also conducted (not shown) and the data converted to a corrosion rate. All of these measurements are compared in Table 1.

Table 1 – Comparison of SmartCET LPR, PAR LPR, and PAR PD (potentiodynamic) corrosion rates.

SmartCET LPR	PAR LPR	PAR PD
0.0028	0.0008	na
1.83	1.63	na
1.79	1.65	1.52
0.66	0.60	0.45
0.44	0.41	0.30
1.44	1.28	0.91
0.15	0.14	0.14

The measurements in Table 1 show a good agreement between the PAR and the SmartCET

LPR corrosion rates. The potentiodynamic (PD) corrosion rates are actually close to the SmartCET LPR corrosion rates, but not quite as good as the PAR LPR corrosion rates. This is to be expected because of the different parameters used to make the PAR LPR and PAR PD measurements.

Electrochemical tests on a coal-ash-covered 304 SS ECR probe, Figure 7, show a more complicated potentiodynamic polarization behavior. Part of the reason for this is that the potential was reversed at 0.5 V vs OCP in order to determine if pitting was occurring.

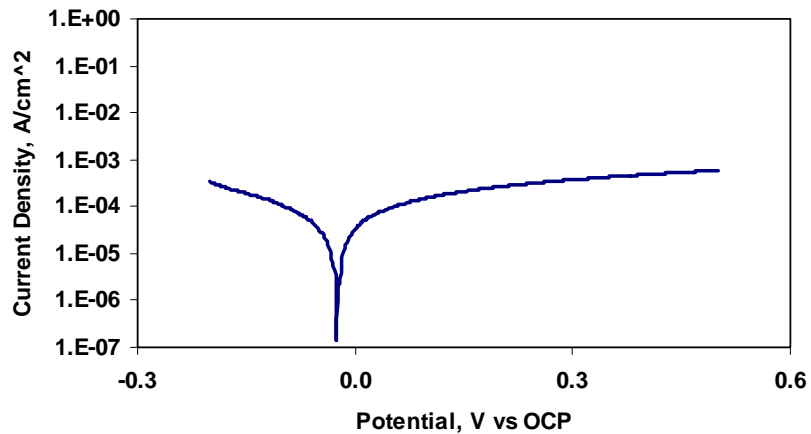


Figure 6 – Potentiodynamic polarization curve of a incinerator-ash-covered 304 SS ECR probe at 500°C.

The polarization curve in Figure 7 suggests active-passive behavior, pitting breakdown (a pitting potential, E_p , and a repassivation potential, E_{rp}). If this proves to be reproducible in future experiments, it supports the pitting factor information reported by the SmartCET unit. Of course, visual examination of the probe will be used to verify the presence of localized corrosion.

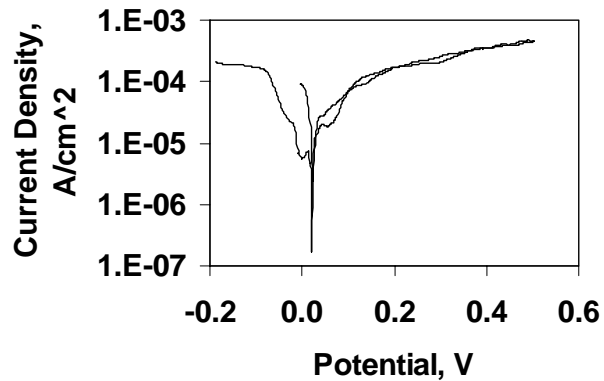


Figure 7 – Potentiodynamic polarization behavior of a coal-ash-covered 304 SS ECR probe at 500°C.

Quantitative Nature Of ECR Probes

One of the key features of corrosion rate probes is that they produce a reading that is can be equivalent to the actual corrosion rate of a structure. This is the meaning of Quantitative Nature. If this is not the case, then it is essential that the signal be proportional in a regular manner to the corrosion rate. This would make the measurements semi-quantitative and would require a calibration curve or factor. The approach to understanding this feature of ECR probes is to use mass loss coupons embedded in ash and exposed at the same time and to the same conditions as the ECR probe. Figure 8 shows a picture of the apparatus that holds the mass loss coupons in the test environment.

Mass loss coupons are removed from the experiment, cleaned of all ash and corrosion deposits and weighed to determine weight loss due to corrosion. Corrosion penetration rates are then calculated using weight loss, exposed area, and exposure time. Electrochemical corrosion rates for the ECR probes were calculated either by: (1) converting corrosion rates to weight loss for each 7 min measurement period, summing the weight losses, and then converting to corrosion penetration rates as above, or (2) calculating an average corrosion rate over the exposure time period. Both techniques give nearly identical results.

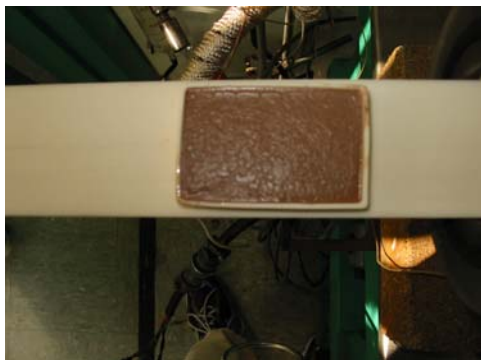


Figure 8 – Ceramic boat containing two ash-embedded mass loss coupons.

Another technique, optical profilometry, is being used to provide further verification of the quantitative nature of ECR probes. While there is no data for this report, plans have been made. Optical profilometry can measure and digitize the surface of materials. If there is a reference point, then it will be possible to measure and calculate the volume of a material lost due to corrosion. This can then be converted into a mass loss and then, as above, a corrosion rate.

For the ECR probes, the reference points are two pieces of alumina embedded at each end of the sensors, and the surface analyzed is typically the center sensor, the reference electrode. The reference electrode sensor is chosen because it most closely resembles the unpolarized mass loss coupons. The counter and working electrode sensors are polarized every 7 minutes during the LPR and HDA measurements. Measurements taken before exposure are subtracted to provide a corrected corrosion volume loss.

SUMMARY/CONCLUSIONS

- ECR probes are responsive to changes in temperature and gas composition. Ash composition does affect this response.
- ECR probes appear to be quantitative based on initial measurements.
- Corrosion reactions occurring in the ash appear to be at least partially electrochemical.
- Both EN and potentiodynamic polarization measurements predict that localized or pitting corrosion occurs for the coal-ash-covered 304 SS ECR probe.

REFERENCES

1. T.M. Linjeville, K.A. Davis, G.C. Green, W.M. Cox, R.N. Carr, N.S. Harding, and D. Overacker, "On-Line Technique for Corrosion Characterization in Utility Boilers, Proceedings of Power Production in the 21st Century: Impacts of Fuel Quality and Operations," United Engineering Foundation, Snowbird, UT, October 28-November 2, 2001.
2. T.M. Linjeville, J. Valentine, K.A. Davis, N.S. Harding, and W.M. Cox, "Prediction and Real-time Monitoring techniques for Corrosion Characterization in Furnaces," Materials at High Temperatures, Vol. 20, No. 2, pp. 175-184, 2003.
3. D.M. Farrell, W.Y. Mok, and L.W. Pinder, "On-line Monitoring of Furnace-Wall Corrosion in a 125 MW Power Generation Boiler," Materials Science and Engineering, Vol. A121, pp. 651-659, 1989.
4. D. M. Farrell, "On-line Monitoring of Fireside Corrosion in Power Plant," 12th International Corrosion Congress, Vol. 12, pp. 4131-4140, 1993.
5. G. Gao, F.H. Stott, J.L. Dawson, and D.M. Farrell, "Electrochemical Monitoring of High-Temperature Molten Salt Corrosion," Oxidation of Metals, Vol. 33, Nos. 1/2, pp. 79-94, 1990.
6. G.J. Bignold and G.P. Quirk, "Electrochemical Noise Measurements in a 500 MW Steam Turbine to Maximize Lifetime Under Changing Operational Demands," Paper no, 02333, CORROSION/2002, NACE International, Houston, TX, 20 pp, 2002.
7. D. A. Eden and B. Breene, "On-Line Electrochemical Corrosion Monitoring in Fireside Applications," Paper No. 03361, CORROSION/2003, NACE International, Houston, TX, 10 pp., 2003.